

Spectroscopic Study of Egyptian Blue Mixed with Other Pigments

by M. Carmen Edreira*, M. José Feliu, Concepción Fernández-Lorenzo, and Joaquin Martín

Department of Physical Chemistry, University of Cádiz, Apdo. 40, E-11510 Puerto Real (Cádiz)

The Romans used a vast array of colors in their mural paints. The applied pigment mixtures containing Egyptian blue resulting in green, ochre, brown, gray, and white hues were studied. The chromatic characterization of wall paintings by electronic spectroscopy provided an easy and reliable procedure for the grouping of the samples to be studied (see *Table*). Subsequent use of other spectroscopic techniques such as *Fourier*-transform (FT) IR and energy-dispersive X-ray spectroscopy (EDS), combined with X-ray diffraction (XRD), led to convenient identification of the pictorial layer components that define and differentiate each chromatic group. Colors impossible to produce with only one pigment can be obtained by mixing Egyptian blue with other pigments. The dominant wavelength is displaced in such way that the artist obtains new tonalities.

1. Introduction. – Egyptian blue is an artificial calcium copper silicate that is made by heating, to *ca.* 850°, a mixture of a calcium compound (such as powdered limestone) with a copper compound (such as malachite) and silica (usually in the form of quartz sand). It was the first synthetic pigment. Because of the coincidence of X-ray-diffraction data of Egyptian blue with the mineral cuprorivaite, the accepted formula for this pigment ($\text{CaCuSi}_4\text{O}_{10}$) is that of cuprorivaite. In antiquity, Egyptian blue was the most frequently used blue pigment in Europe from the early Egyptian dynasties until the end of the Roman period. After the Roman period, Egyptian blue was rarely used [1][2]. In the literature, we can find various studies on the production of this pigment and on its use as a blue pigment in different works of art [1–9].

The use of Egyptian blue to produce different tonalities by its addition to other pigments is studied in this work. The results of nine samples of *Pinturas Báquicas* of the 2nd century A.D. from the building *Casa del Mitreo* are shown. These results are compared with the twelve samples from the buildings *Cripta del Museo* and *Alcazaba*, of the 1st century A.D. [9], and with the *Pinturas Báquicas* from *Casa del Mitreo* [10][11] whose similar colors have been obtained without addition of Egyptian blue. All the samples were in a good conservation state, and they were made available to us by the *Museo Nacional de Arte Romano de Emerita Augusta*, Mérida (Badajoz, Spain).

Using light microscopy, we observed the homogeneity of the Egyptian-blue-grains distribution in the samples, which means that they are artificial mixtures and that the presence of the pigment is not the result of an accidental contamination.

The study of mural-painting samples involves the characterization of the pictorial surface, which is constituted of the pigment and the substrate in which it is immersed. The chemical composition of both materials offers significant information on the techniques that were used in its creation. In this way, spectroscopic techniques were applied to pictures, allowing chromatic characterization and identification of the pigments present.

2. Experimental. – All samples were studied by selected techniques according to the results of previous works [9–13].

2.1. *Chromatic Characterization.* In this work, an objectively reproducible chromaticity characterization was carried out by electronic spectroscopy. The method consisted of determination of the optical reflectance in the VIS-frequency range by means of an *Otsuka-MCPD-1100* VIS/UV spectrophotometer. The system was equipped with optical-fiber light-conducting elements that allowed direct study of the pictorial surface of the material without perturbing it.

The chromaticity coordinates x_{10} and y_{10} , deduced from the tristimulus values X_{10} , Y_{10} , Z_{10} , were calculated by the normalized CIE64 system [14–16]. These variables, which define the tonality and color saturation, were represented in the color-space diagram. An incandescent tungsten lamp with filtered emission was used as the illumination system, and the CIE illuminant was the standard source D_{65} . As the white pattern, a low-pressure compressed tablet of chemically pure magnesium oxide powder was used. The reflectivity of this substance is *ca.* 97–98% (*Erb* and *Budde* [17]), and it is chemically stable. The sample chamber had a normalized geometry of $0^\circ/45^\circ$ for the illumination/observation process to minimize the specular/diffuse reflectance ratio of the captured radiation and to obtain a realistic chromaticity value.

2.2. *Chemical Analysis.* The chemical identification of the pictorial and substrate substances was performed by means of energy-dispersive X-ray spectroscopy (EDS), *Fourier-transform* IR and X-ray-diffraction (XRD) techniques. For elemental analysis, a *LINK AN10000* energy-dispersive X-ray detector system connected to a *JEOL JSM820* scanning electron microscope was used. The samples were gold-coated to prevent surface charging, thus, a constant gold signal appears in all the EDS plots.

A *Nicolet Impact-410-FT-IR* spectrophotometer with *OMNIC* software was used to obtain molecular information. The spectral analysis was performed by searching a total of 40000 spectra in several commercial libraries, including those of the *U.S. Geological Survey Minerals*, *Commercial Material Painter Minerals*, *Sigma Dyes, Stain and Natural Pigments*, *Aldrich Condensed Phase and Coating Technology*. In all cases, the XRD technique was used to confirm that the crystal structures were of the same molecular compound.

3. Results. – 3.1 *Preamble.* In this work, the abbreviations *mi*, *cr*, and *al* are the general names that we associate with the samples from the buildings *Casa del Mitreo*, *Cripta del Museo*, and *Alcazaba*.

A *ca.* 1-mm thick layer forms the pictorial surface of all samples. Calcite, a crystallographic variety of calcium carbonate, is detected in the binder of all samples, along with varying amounts of common impurities, which may include quartz, dolomite, *etc.* This establishes that the paintings have been made by the ‘fresco painting’ technique, *i.e.*, with lime mortar. Typical components of standard silicates are present in many cases. These silicates are associated with aggregates due to the mortar, dust, and burial remains, and, only in some cases, to the pigment used for coloring the layer.

The reflectance spectra of the pictorial surface of all samples were registered in the VIS range over some zones (illumination-spot size *ca.* 3 mm in diameter) for each one of the different samples, thus furnishing a statistically representative value. The colorimetric coordinates x_{10} , y_{10} , Y_{10} , the saturation, and the dominant wavelength achieved are summarized in the *Table*. A 3D graphic with x_{10} , y_{10} , and Y_{10} is shown in *Fig. 1* and the projection of this graph in the *XY* plane or CIE64 diagram in *Fig. 2*. Enlargements of this diagram in the interesting zones are presented below in *Figs. 7, 12, 16, and 27*. With regard to the chromatic coordinates and the saturation values, they seem to be very close to the neutral white. This behavior is fitting to the Roman mural paintings because of the small concentration of pigments in the pictorial layer [18].

The samples appear clearly grouped in five zones. The terms used for denoting these groups are based on the human visual sensation of colors; in spite of the chromaticity, values obtained can indicate small discrepancies. So, the zones are denoted as greenish colors, ocher colors, brown colors, gray colors, and white colors. The results obtained

Table. General Characteristics of the Samples Studied^{a)}

Group	Sample	Chemical composition		Chromatic coordinates			$\lambda_{\text{dominant}}$ [nm]	Saturation [%]
		Pigment	Base	x_{10}	y_{10}	Y_{10}		
Greenish colors	<i>mi1</i>	Egyptian blue, goethite	CaCO ₃	0.3227	0.3611	21.138	557	10.0
	<i>mi2</i>	green earth	CaCO ₃	0.3451	0.3608	27.174	571.5	17.6
	<i>cr1</i>	green earth	CaCO ₃	0.3335	0.3505	33.239	571	11.1
	<i>cr2</i>	green earth	CaCO ₃	0.3225	0.3489	37.655	562	7.9
	<i>all</i>	green earth	CaCO ₃ /CaSO ₄	0.3498	0.3433	18.818	586	14.1
Ocher colors	<i>mi3</i>	goethite, Egyptian blue, cinnabar	CaCO ₃	0.3976	0.3873	21.153	577	39.5
	<i>mi4</i>	goethite, Egyptian blue, cinnabar	CaCO ₃	0.3935	0.3698	18.699	581.5	37.5
	<i>mi5</i>	goethite, cinnabar, Egyptian blue	CaCO ₃	0.4093	0.3734	22.545	582.5	27.2
	<i>mi6</i>	goethite	CaCO ₃	0.3765	0.3616	29.352	581.5	26.3
	<i>cr3</i>	goethite	CaCO ₃	0.4143	0.3834	32.992	580	43.8
	<i>cr4</i>	goethite	CaCO ₃	0.3745	0.3601	54.696	582	27.5
Brown color	<i>mi7</i>	hematite, Egyptian blue	CaCO ₃	0.3527	0.3552	15.513	578	18.4
Gray colors	<i>mi8</i>	Egyptian blue, iron oxides	CaCO ₃	0.3117	0.3363	30.181	–	–
	<i>mi9</i>	Egyptian blue, iron oxides	CaCO ₃	0.3196	0.3406	26.618	–	–
	<i>a12</i>	carbon black	CaCO ₃ /CaSO ₄	0.3261	0.3335	25.370	–	–
White colors	<i>mi10</i>	calcite, Egyptian blue	CaCO ₃	0.3530	0.3598	40.101	575	21.0
	<i>mi11</i>	calcite, Egyptian blue	CaCO ₃	0.3452	0.3531	50.881	576	15.8
	<i>mi12</i>	calcite	CaCO ₃	0.3667	0.3662	60.005	577	25.0
	<i>cr5</i>	Calcite	CaCO ₃	0.3491	0.3548	59.019	578	18.4
	<i>cr6</i>	calcite	CaCO ₃	0.3521	0.3501	45.318	577	18.4
	<i>cr7</i>	calcite	CaCO ₃	0.3496	0.3574	79.990	576	18.4

^{a)} The main compounds of the pigmentary layer and binder are shown. The chromatic coordinates x_{10} and y_{10} , luminosity Y_{10} , dominant wavelength, $\lambda_{\text{dominant}}$, and saturation of each sample are listed.

are described below for each of the groups. The colorimetric data, preceded by the chemicominalogical composition are shown in the *Table*. This composition was obtained by using the aforementioned analytical techniques.

3.2. *Greenish Colors*. The most common way to obtain the green color in Roman mural paintings is by using the so-called ‘green earth’ pigment [9–11][18][19]. According to *Delamare* [19], the name ‘green earth’ encompasses a mixture of clays, the most important of which are glauconite, celadonite, and the chlorite group (clinocllore and penninite); all of them are aluminium silicates with impurities of Fe²⁺, Fe³⁺, K⁺, and other ions. The green earth is the most abundant pigment of samples in the *mi2*, *cr1*, *cr2*, and *all*. As an example, the FT-IR spectrum of the *all* sample is shown in *Fig. 3*. Bands indicating the presence of calcium carbonate compounds, calcium

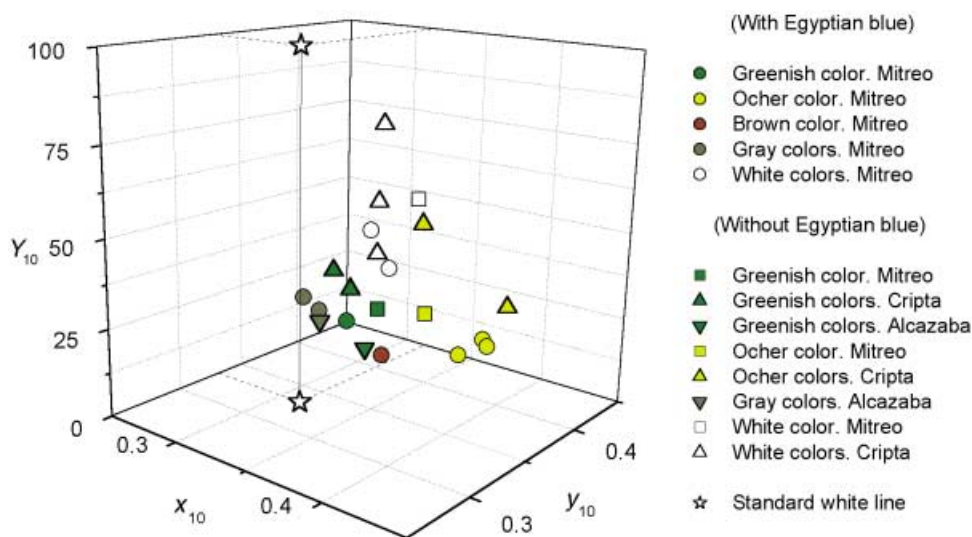


Fig. 1. 3D Graphic of the chromatic coordinates measured for the 21 samples studied. Five groups of samples can be observed, each one associated with human chromatic sensations.

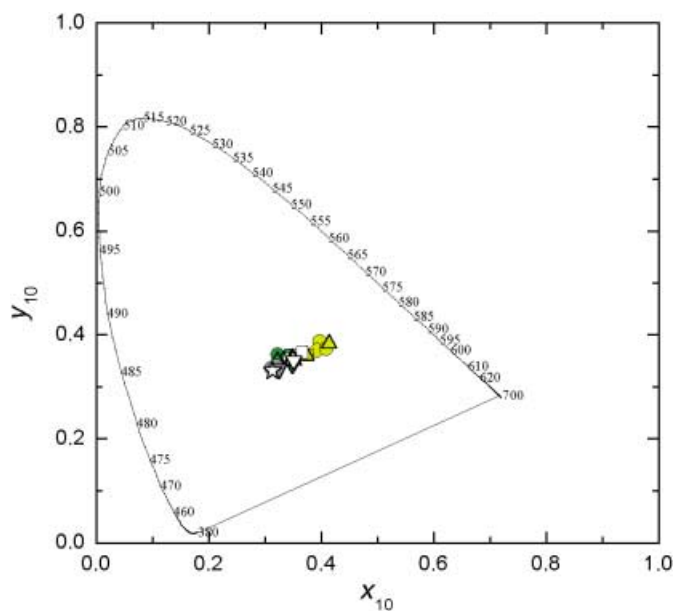


Fig. 2. CIE64 Chromaticity diagram showing the dominant wavelength of all the samples

sulfate (gypsum), and clinocllore (green earth) are detected. This last compound is characterized by a small band at 662 cm^{-1} , a broad band with two maxima at 978 and 1009 cm^{-1} overlapping with some gypsum and calcium carbonate peaks, and a band at

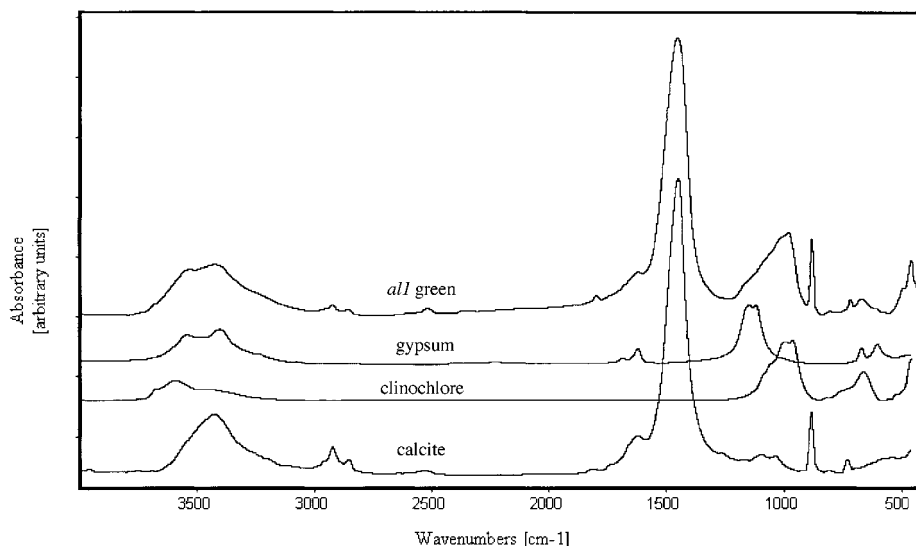


Fig. 3. FT-IR Spectrum of the all green sample. Besides the typical substances of the binder, clinochlore as a pigment of the pictorial surface can be detected.

3406 cm⁻¹ with two shoulders at 3549 and 3680 cm⁻¹. The characterization was complemented by XRD measurements. As an example, the diffractogram of the cr2 sample shown in Fig. 4 reveals, apart from quartz, calcite, and some silicates, the presence of green earth as glauconite.

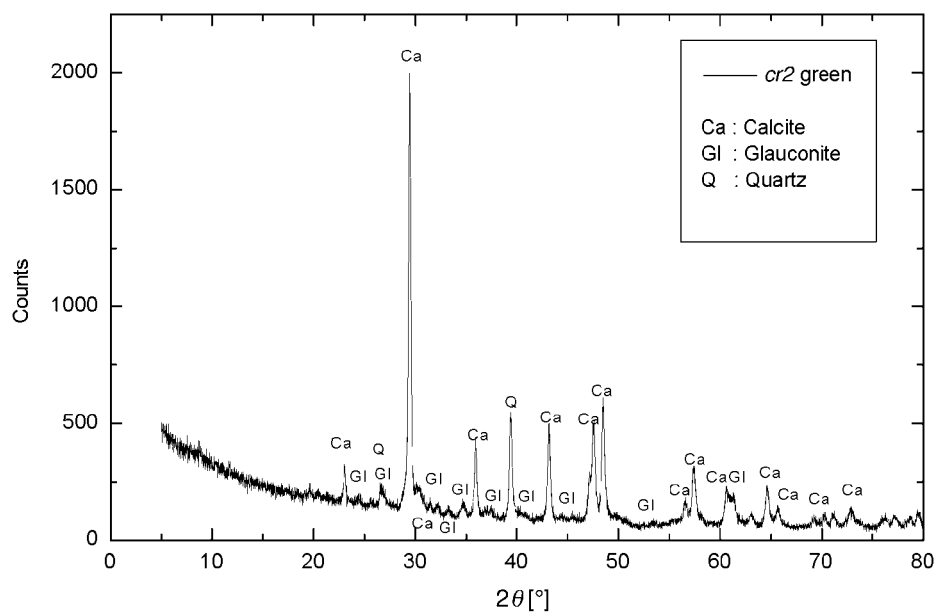


Fig. 4. X-Ray diffractogram of the cr2 green sample. Glauconite, calcite, and quartz are detected.

On the contrary, the XRD of the *mi1* sample, which also has a green color, shows the presence of cuprorivaite and yellow iron oxides (*Fig. 5*). Most of the latter are in the goethite form. In the FT-IR spectrum of the *mi1* sample (*Fig. 6*), the bands associated with the presence of calcite (bands at 2515, 1439, 874, and 705 cm^{-1}), Egyptian blue (bands at 1160, 1079, 1054, and 1009 cm^{-1}), and yellow iron oxides (bands at 912 and 799 cm^{-1}) are detected.

These results indicate that the green coloration of the *mi1* sample is not due to green earth, but to a mixture of Egyptian blue and yellow iron oxides (goethite).

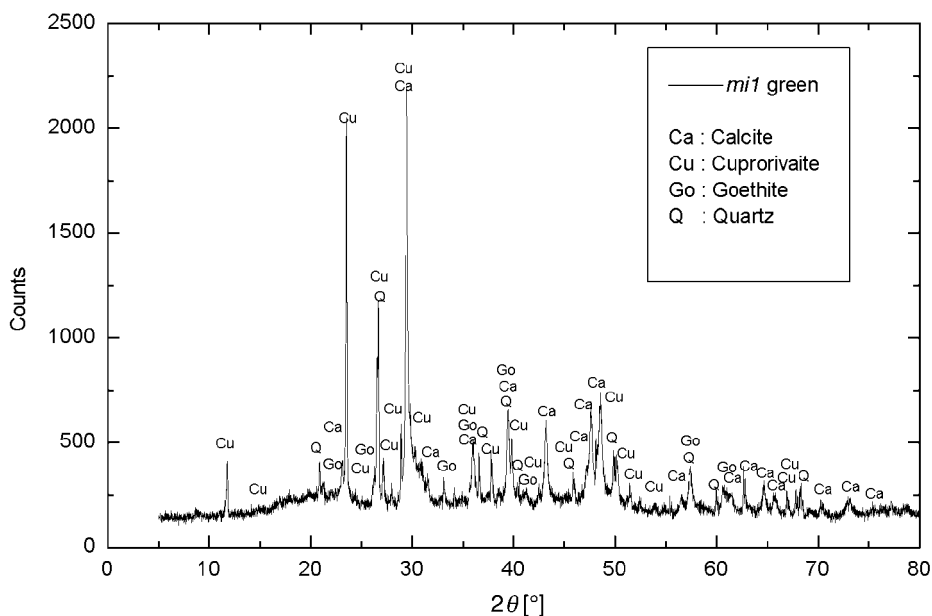


Fig. 5. X-Ray diffractogram of the *mi1* green sample. Cuprorivaite, goethite, calcite, and quartz are detected.

The chromatic characterization (*Table, Fig. 7*) also shows substantial differences, between the samples of the greenish-color group, the *mi1* sample presenting a lower dominant wavelength than the other samples and a lower luminosity. Thus, the color varies from a green tonality for the *mi1* sample to a yellowish-green tonality for the samples whose pigment is exclusively constituted by green earths.

3.3. *Ocher Colors*. Six samples that present this color were studied: *mi3*, *mi4*, *mi5*, *mi6*, *cr3*, and *cr4*. In the IR spectrum of the *cr4* sample (*Fig. 8*), calcite (bands at 2515, 1439, 874, and 705 cm^{-1}), common clayey silicates like illite (band at 1027 cm^{-1} with a shoulder at 1092 cm^{-1}), and yellow iron oxide (bands at 912 and 799 cm^{-1}) are identified. This last compound is considered to be the pigment that defines the sample color. Some of the band shapes are due to the sum of more than one vibrational band of the aforementioned compounds (*i.e.*, the broad band at 3425 cm^{-1} with a shoulder at 3180 cm^{-1}). The diffractogram of the *cr4* sample (*Fig. 9*) establishes that its pigment consists only of goethite. Similar results were obtained for the *mi6* and *cr3* samples.

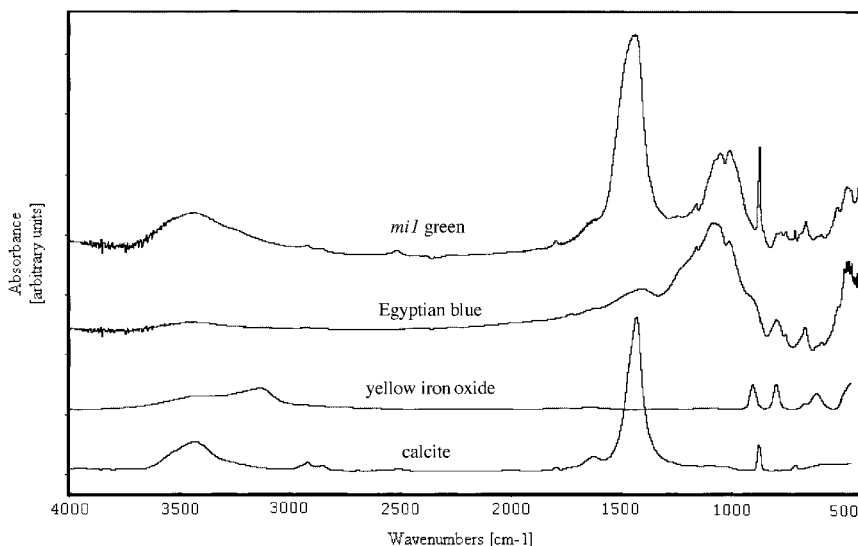


Fig. 6. FT-IR Spectrum of the mil green sample. Besides the typical substances of the binder, Egyptian blue and yellow iron oxide as pigments of the pictorial surface can be detected.

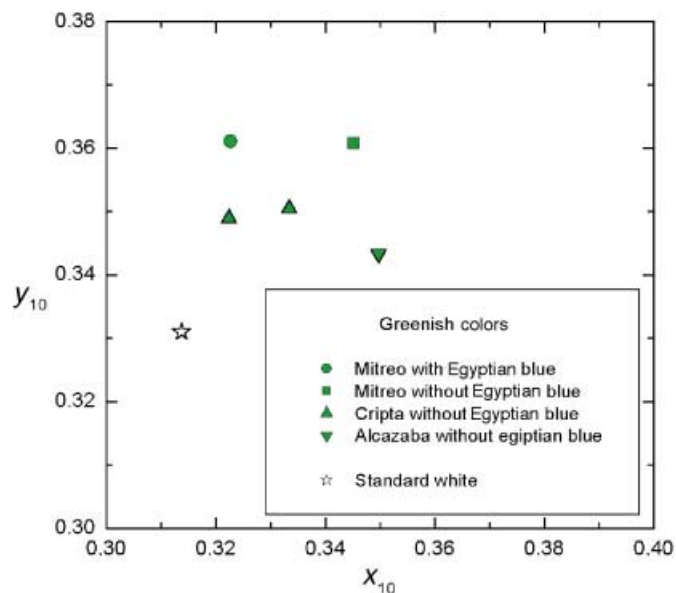


Fig. 7. CIE64-Chromatic-diagram enlargement of Fig. 2 for the green samples

There are some differences between the *mi3*, *mi4*, and *mi5* samples. For example, the XRD analysis of the *mi4* sample (Fig. 10) reveals the presence of goethite and small quantities of Egyptian blue and cinnabar, apart from quartz, calcite, and some silicates detected. The IR spectrum of the *mi5* sample (Fig. 11) shows bands for calcite (at 2515,

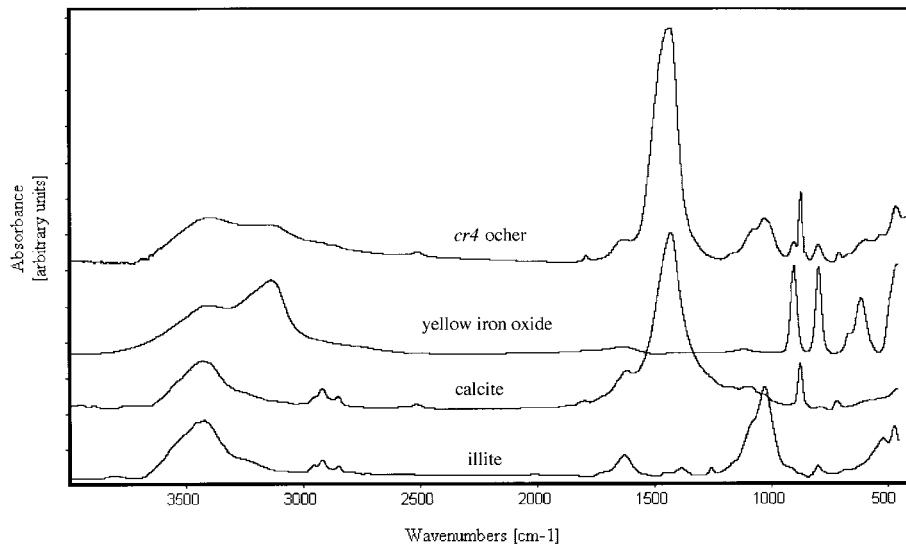


Fig. 8. FT-IR spectrum of the cr4 ocher sample. Besides the typical substances of the binder, yellow iron oxide as pigment of the pictorial surface can be detected.

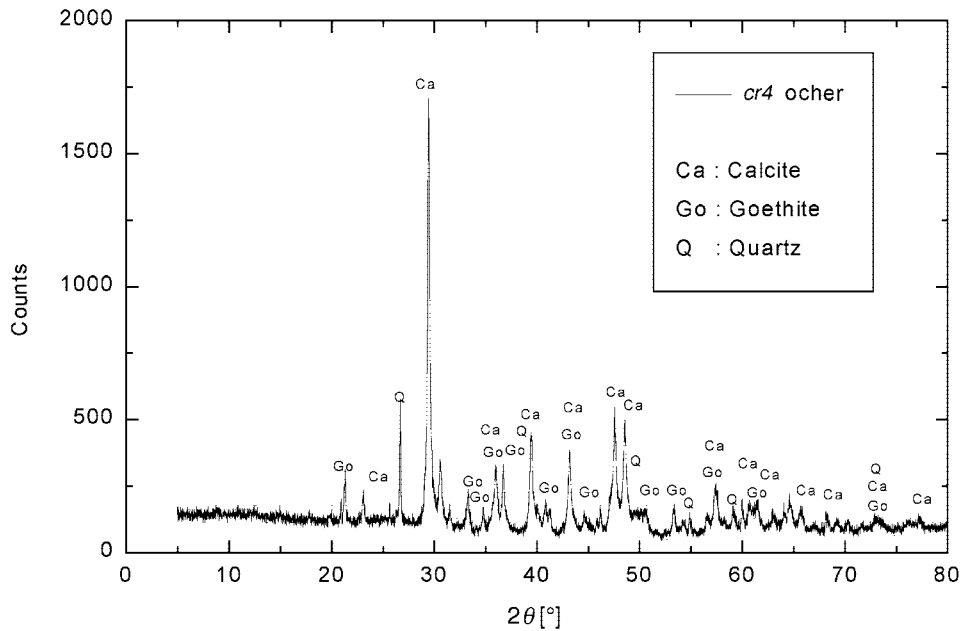


Fig. 9. X-Ray diffractogram of the cr4 ocher sample. Goethite, calcite, and quartz are detected.

1439, 874, and 705 cm^{-1}) and yellow iron oxides (at 912 and 799 cm^{-1}). On the other hand, the band at 1027 cm^{-1} with the shoulder at 1092 cm^{-1} that is attributed to illite has a modified shape due to the presence of Egyptian blue (bands at 1160 , 1079 , 1054 , and

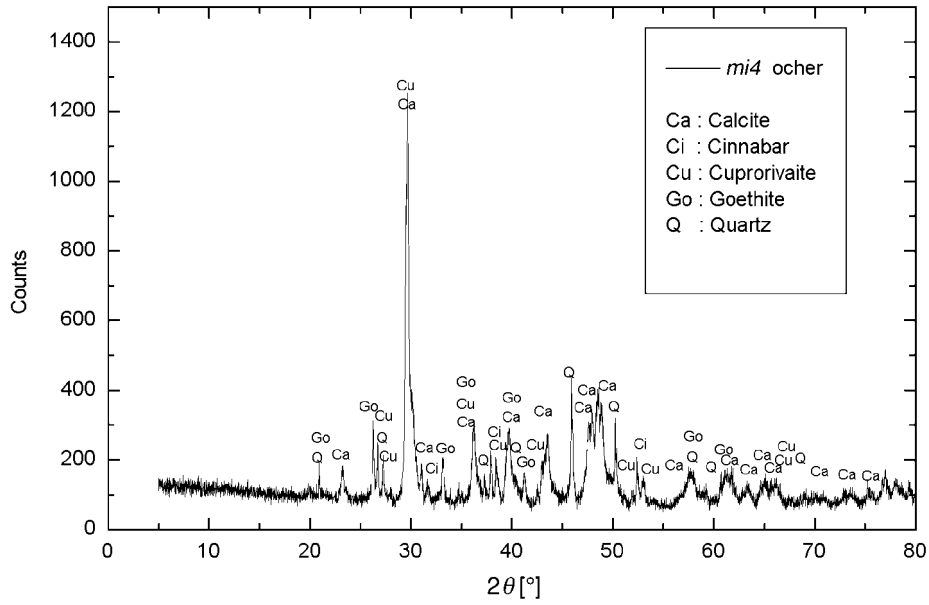


Fig. 10. X-Ray diffractogram of the *mi4 ocher* sample. Goethite, cuprorivaite, cinnabar, calcite, and quartz are detected.

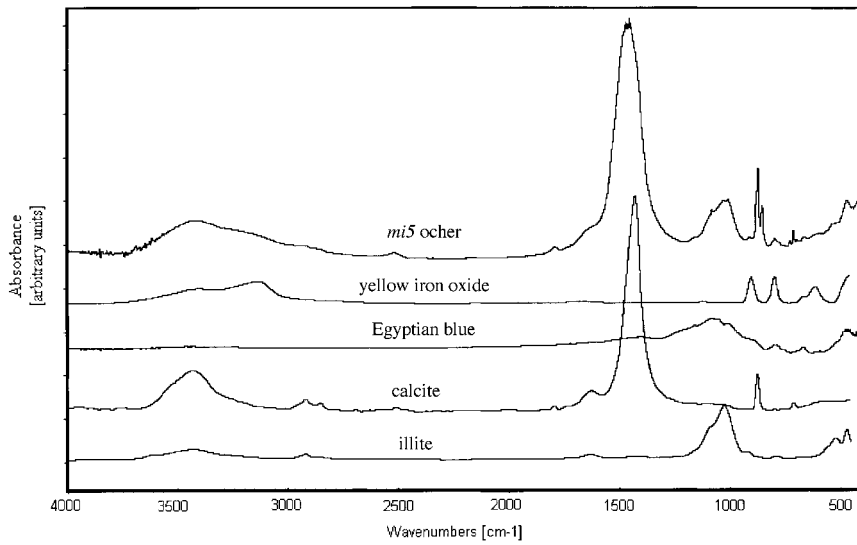


Fig. 11. FT-IR Spectrum of the *mi5 ocher* sample. Besides the typical substances of the binder, yellow iron oxide and Egyptian blue as pigments of the pictorial surface can be detected.

1009 cm^{-1}). Bands due to cinnabar are not observed because they are transparent to IR irradiation.

The chromatic characterization of the six samples of the ocher-color group (Table, Fig. 12) reveals a medium saturation and a dominant wavelength situated at *ca.* 581 nm. The samples containing only goethite as pigment exhibit a medium wavelength of 581.2 nm. The wavelength variation of the Egyptian blue and cinnabar samples *mi3*, *mi4*, and *mi5* can be explained by variations of the proportion of these two minority components. Therefore, the wavelength of the *mi4* sample, which has the same value as the *mi6* sample containing only goethite, decreases towards the greenish yellow zone for the *mi3* sample with an increased proportion of Egyptian blue. The dominant wavelength of the latter sample presents the lowest value in this group ($\lambda_{\text{dominant}}$ 577 nm). On the contrary, when the Egyptian blue proportion decreases and the cinnabar content increases, a rise of the dominant wavelength towards the reddish yellow zone is observed, as in the case of the *mi5* sample, which exhibits the highest value of $\lambda_{\text{dominant}}$ (582.5 nm).

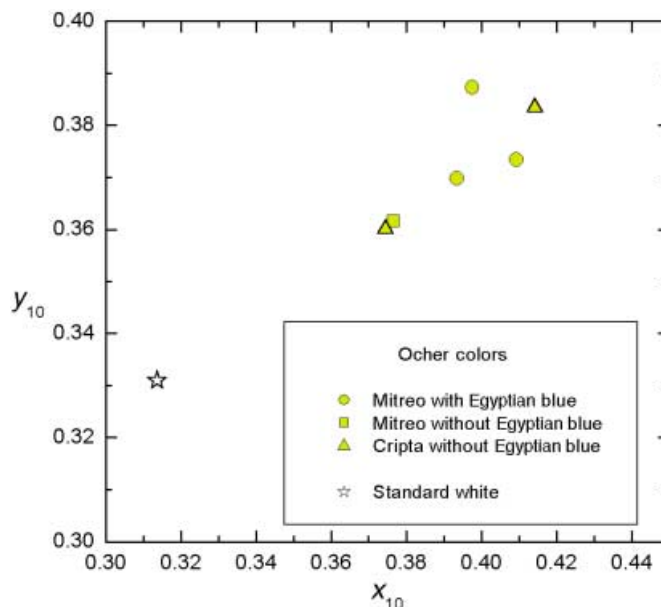


Fig. 12. CIE64-Chromatic-diagram enlargement of Fig. 2 for the ocher samples

The saturation values are similar in all the samples; however, lower luminosity values are observed in the samples containing Egyptian blue.

3.4. *Brown Color.* This group consists of only the *mi7* sample, and there are no comparison samples for this color. Over a reddish-ocher background, many blue crystals are detected by light-microscopy observation (Fig. 13). The general EDS of the *mi7* sample shows the presence of silicon, calcium, and iron apart from the constituent elements of Egyptian blue (silicon, calcium, copper).

The FT-IR spectrum of the *mi7* sample (Fig. 14) establishes the presence of iron oxide in the hematite form (bands at 642 and 534 cm^{-1}), Egyptian blue (bands at 1160,

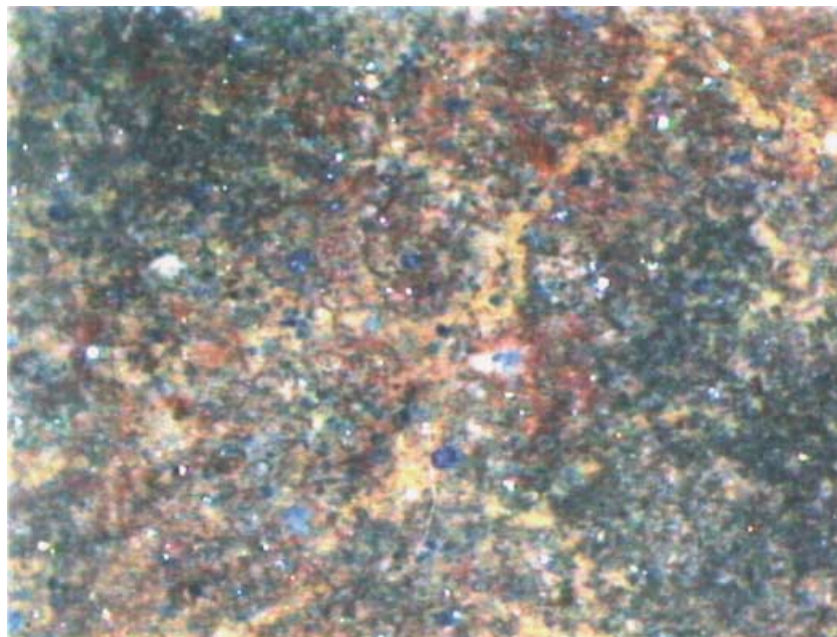


Fig. 13. Binocular-magnifier sight of the brown mi7 sample. Many blue crystals are observed.

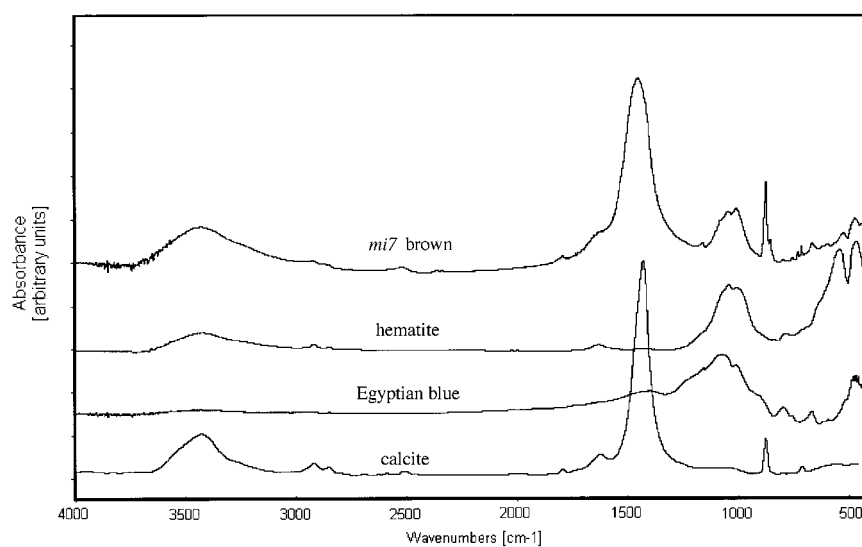


Fig. 14. FT-IR Spectrum of the mi7 brown sample. Besides the typical substances of the binder, hematite and Egyptian blue as pigments of the pictorial surface can be detected.

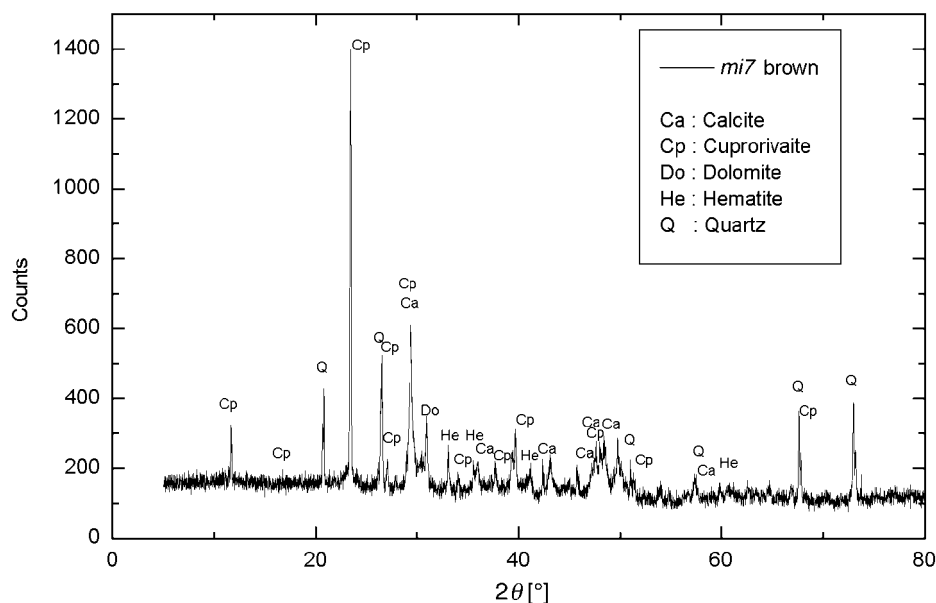


Fig. 15. X-Ray diffractogram of the *mi7* brown sample. Hematite, cuprorivaite, dolomite, calcite, and quartz are detected.

1079, 1054, and 1009 cm^{-1}), and calcite (bands at 2515, 1439, 874, and 705 cm^{-1}). These results were corroborated by XRD measurements (Fig. 15).

The chromatic values for the *mi7* sample confirm that the addition of Egyptian blue to the hematite red pigment decreases the dominant wavelength towards lower values, setting it into the ochre zone.

3.5. Gray Colors. The samples *mi8*, *mi9*, and *al2* constituting this group have very low saturation values (Table, Fig. 16), i.e., they provide an achromatic stimulus corresponding to the visual interpretation of whites, grays, or blacks. These achromatic stimuli are different from each other due to different luminosity values, and their visual interpretation is gray. This low saturation can be achieved by two different methods: by a low pigment concentration in a white binder, or by adding any pigment that desaturates the color of the predominant pigment [14][15].

The *al2* sample of gray color is a clear example of low saturation obtained by the first method, where the pigment is black carbon in a matrix of several white compounds. Indeed, its FT-IR spectrum (Fig. 17) exhibits absorptions of calcium carbonate compounds (bands at 3425, 2515, 1439, 874, and 705 cm^{-1}), gypsum (bands at 3544, 3405, 1150, and 1121 cm^{-1}), and basic silicates (band at 1027 cm^{-1}) but no bands associated with an organic or inorganic pigment. Because graphite and amorphous carbon cannot be detected by the FT-IR technique, the XRD of the *al2* sample was recorded, which confirms the presence of the aforementioned matrix compounds and also of a very little quantity of carbon in the form of graphite (Fig. 18). However, the intensity of the band is too little to generate all the color, thus, the existence of another carbon morphology as amorphous carbon is feasible.

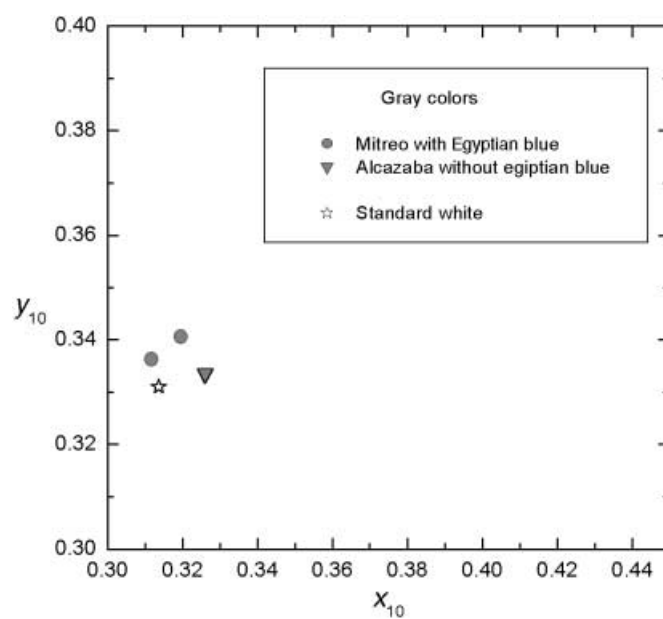


Fig. 16. CIE64-Chromatic-diagram enlargement of Fig. 2 for the gray samples

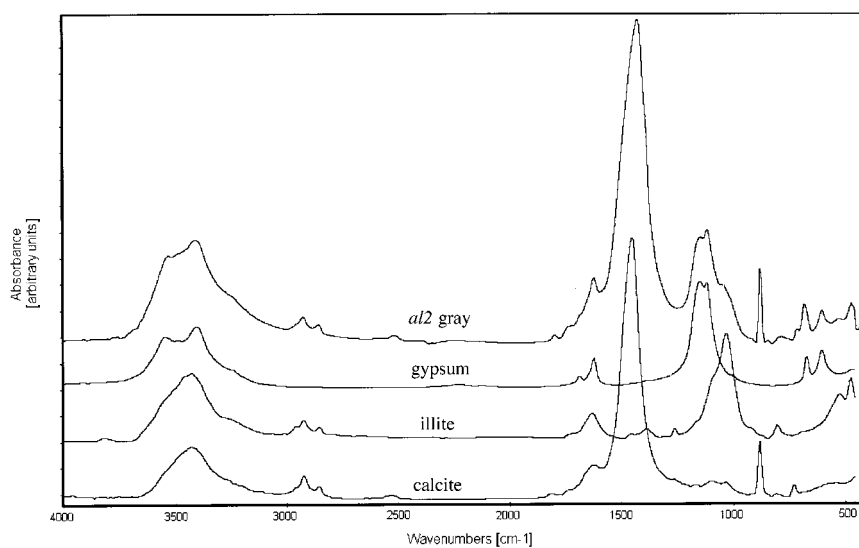


Fig. 17. FT-IR Spectrum of the al2 gray sample. A mixture of calcite, gypsum, and such common silicates as illite can be detected.

The production of gray color by the second method is suggested by the analyses of the other two samples (*mi8* and *mi9*). Optical microscopy reveals many blue crystals over a reddish background (Fig. 19). The EDS confirm the presence of silicon, calcium, copper, and small quantities of iron. The presence of the first three elements is an

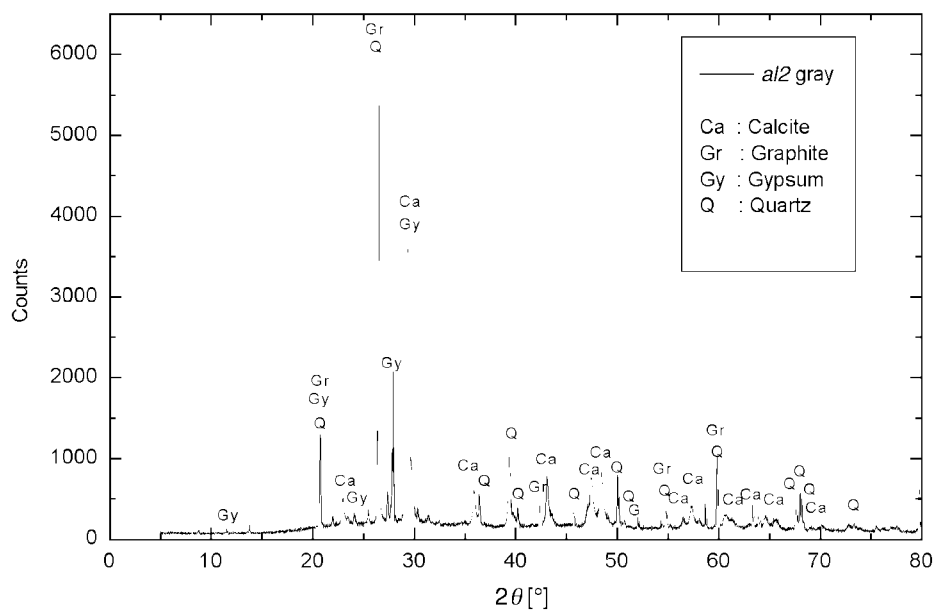


Fig. 18. X-Ray diffractogram of the al2 gray sample. Graphite, calcite, gypsum, and quartz are detected.

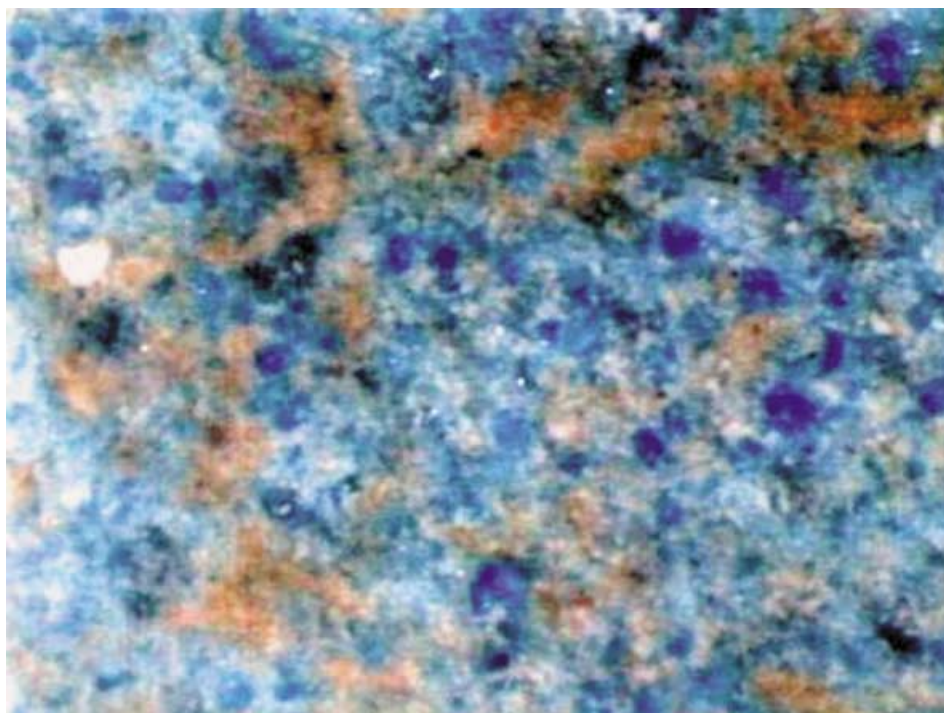


Fig. 19. Binocular-magnifier sight of the mi8 sample. Many blue crystals of different sizes over an ochre background are observed. The normal sight matches a gray color.

indication of the existence of Egyptian blue and that of the fourth for that of iron oxides. Some Egyptian blue crystals of the sample *mi9* are shown in *Fig. 20*, obtained by electron microscopy in the back-scattering mode.

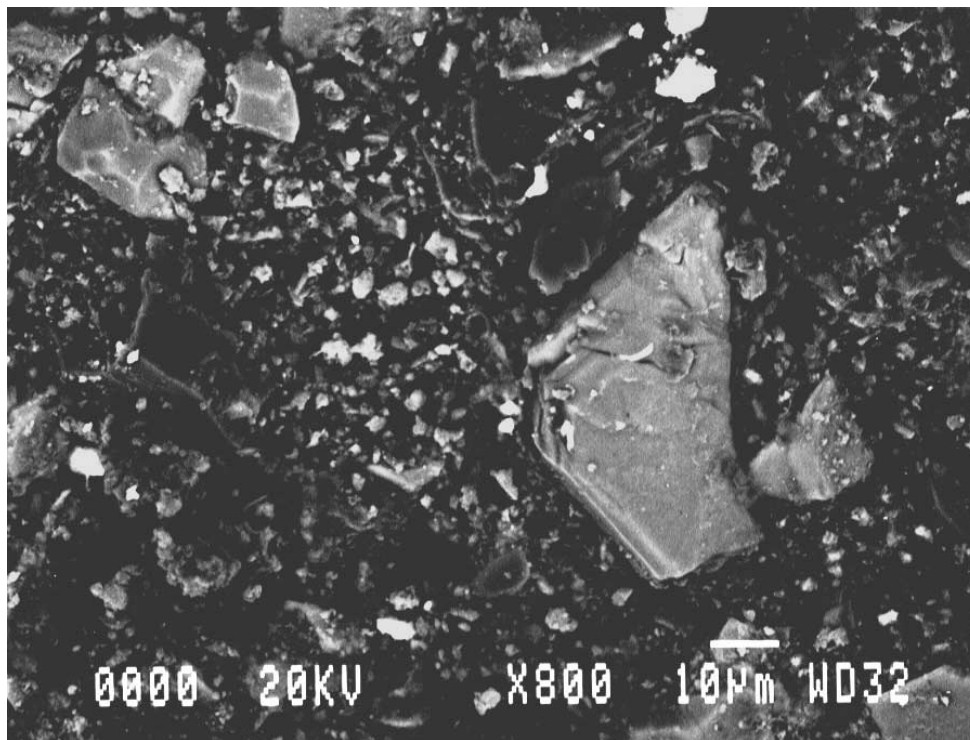


Fig. 20. Back-scattering image of Egyptian blue crystals observed in the *mi9* gray sample

All of these compounds are detected by XRD techniques, where the iron oxide appears in the maghemite-C or hematite form. The mixture of Egyptian blue and iron oxides pigment generates an achromatic stimulus.

3.6. *White Colors*. The *mi10*, *mi11*, *mi12*, *cr5*, *cr6*, and *cr7* samples form this group. In the last four samples, no specific pigments associated with the white chromatic sensation are detected, except for calcium carbonate. The presence of this compound in several morphologies was confirmed by the EDS spectrum (*Fig. 21*) and FT-IR spectrum (*Fig. 22*).

On the other hand, the *mi10* and *mi11* samples, observed by light microscopy, present a pale appearance with other color grains, blue crystals, and a small quantity of red crystals. The presence of the chemical elements of Egyptian blue (*Fig. 23*) and cinnabar (*Fig. 24*) in these crystals are established by EDS. The XRD shows the presence of quartz, white silicates, calcite, and dolomite as basic constituents of the pigmentary layer as well as a minor presence of goethite and cinnabar for the red crystals and Egyptian blue for the blue crystals (*Fig. 25*).

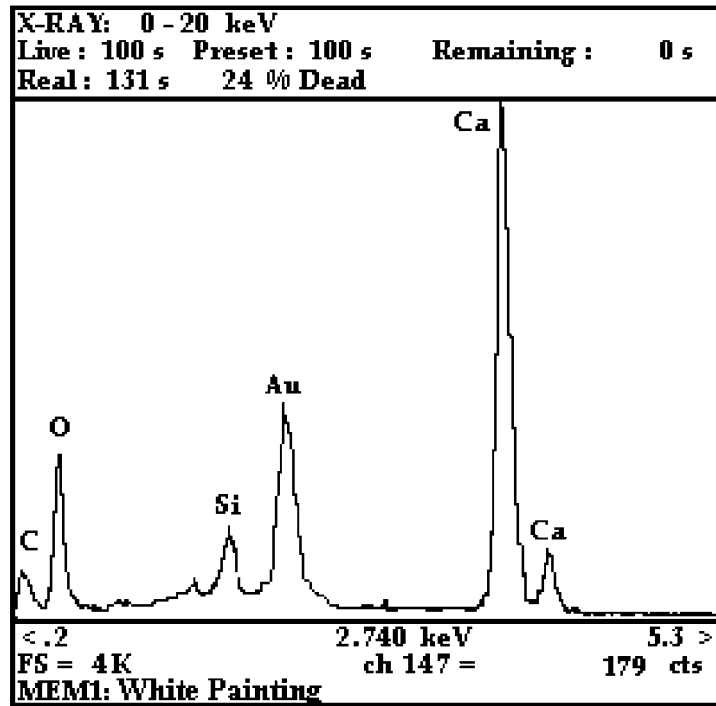


Fig. 21. EDS Plot of a white-painting sample. Ca, O, and C, indicating the presence of CaCO_3 , are observed.

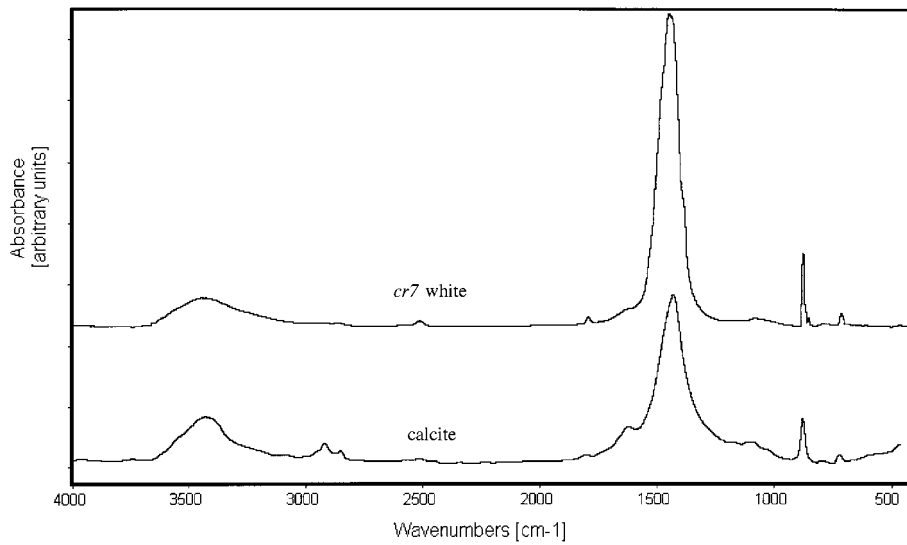


Fig. 22. FT-IR Spectrum of the cr7 white sample. Only calcite is detected, and no other pigment is present.

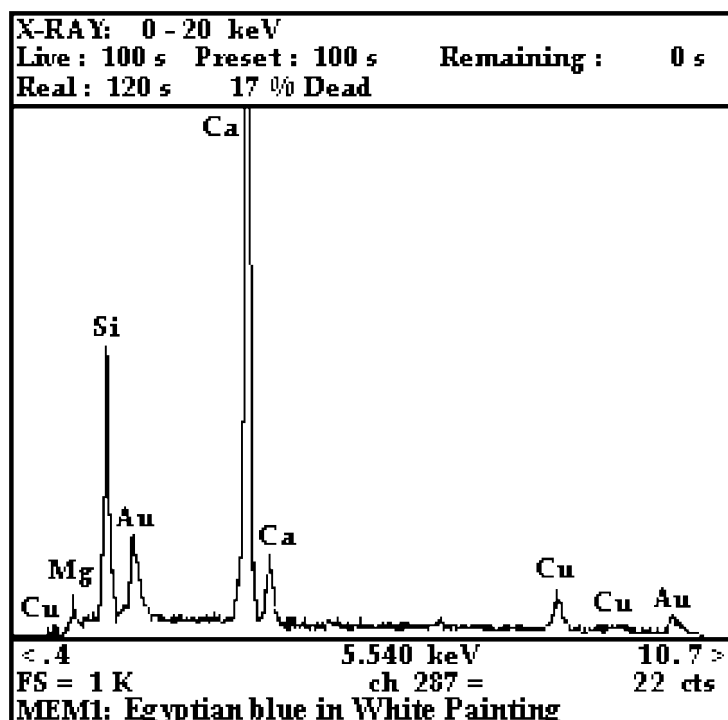


Fig. 23. EDS Plot of a blue crystal of the *mi11* white-painting sample. Ca, Cu, and Si, indicating the presence of Egyptian blue, and Mg and Ca, indicating the presence of carbonates, are observed.

The IR spectrum of the *mi11* sample (Fig. 26) confirms the above-deduced composition. Thus, the 2515, 1439, 874, and 705 cm^{-1} bands can be attributed to the sum of the respective bands of calcium carbonate (calcite) and magnesium calcium carbonate (dolomite), and the 1027 cm^{-1} band with the shoulder at 1092 cm^{-1} to the sum of the band contributions of Egyptian blue and common silicates (illite). The shape of other bands is due to the sum of contributions from all the aforementioned compounds.

The chromatic characterization (Table, Fig. 27) reveals a dominant wavelength between 575 and 578 nm for all the samples of this group indicating that they are actually situated in the yellow zone, but the saturation and luminosity values cause a white visual sensation.

A white sensation can be achieved by increasing the luminosity for similar saturation values or by decreasing the saturation for similar luminosity values. Therefore, the high sensation of white for the *cr7* sample is due to a high luminosity ($Y_{10} = 79.9$) and a low saturation (18.4%), whereas the remaining *cr5* and *cr6* samples from *La Cripta*, exhibiting a medium luminosity, present a more grayish appearance. The *mi12* sample from *Casa del Mitreo*, has also a medium-high luminosity value but a higher saturation than all the other samples of this group, thus providing a yellowish-white visual sensation.

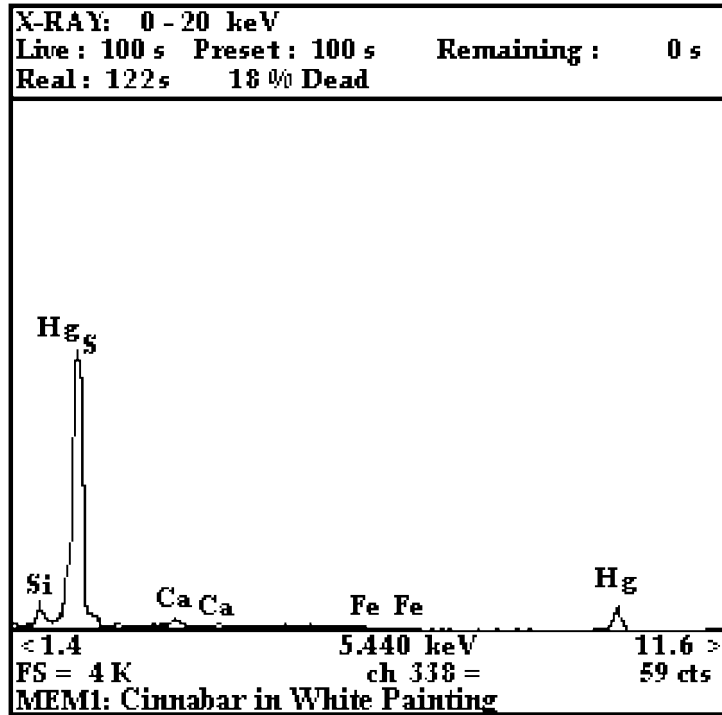


Fig. 24. EDS Plot of a red crystal of the mi10 white-painting sample. S and Hg, indicating the presence of cinnabar, are observed.

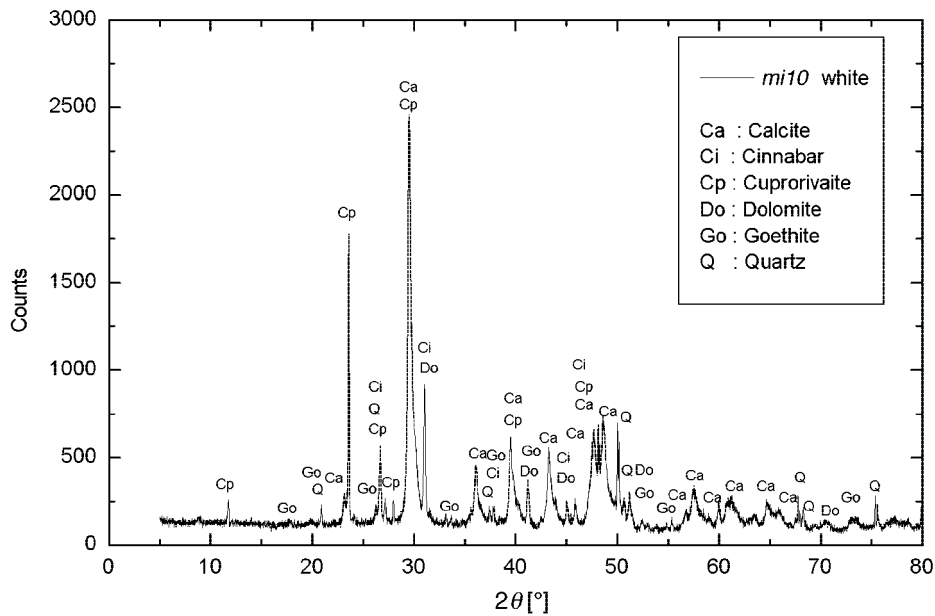


Fig. 25. X-Ray diffractogram of the mi10 white sample. Calcite, dolomite, cuprorivaite, cinnabar, goethite, and quartz are detected.

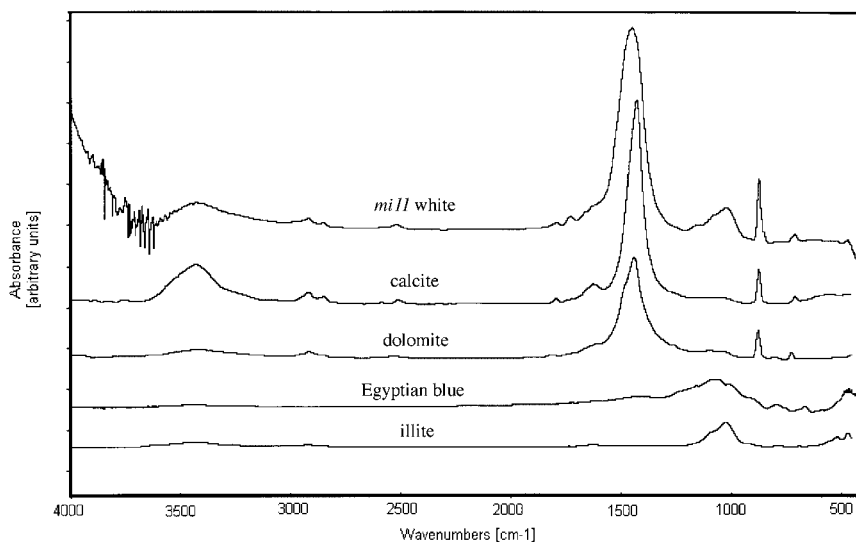


Fig. 26. FT-IR Spectrum of the *mi11* white sample. The main compounds detected are calcite, dolomite, Egyptian blue, and illite. The first one is associated with the pigment.

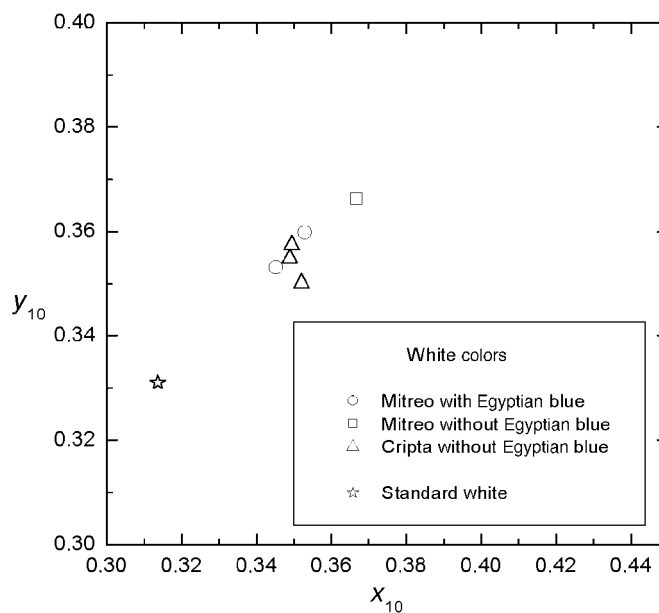


Fig. 27. CIE64-Chromatic-diagram enlargement of Fig. 2 for the white samples

The addition of Egyptian blue to the white pigment, as in the *mi10* and *mi11* samples, causes a decrease of the color saturation (having a minor luminosity) compared to the other white samples and is more marked in *mi11*. Therefore, this sample is the nearest to the white visual sensation (having a medium luminosity). We

suppose that the addition of Egyptian blue has been made to achieve a higher intensity of the white sensation.

4. Conclusions. – Twenty-one samples from *Pinturas Báquicas* of *Casa del Mitreo*, *Cripta del Museo*, and *Alcazaba* were studied, identifying the nature of the pigments in the samples. The chromatic characteristics of the samples measured by reflectance spectroscopy in the VIS region were also determined, and then a normalized process of chromatic coordinate calculus, defined by CIE64, was applied.

We found that the Egyptian blue pigment has been used for the production of different colors by mixing it with other inorganic pigments; in particular, the following colors have been produced:

- a) green hues by mixing Egyptian blue with yellow iron oxides (goethite);
- b) yellow and ocher colors from yellow iron oxides such as goethite by adding small quantities of Egyptian blue and cinnabar to make these colors brighter and to modify the goethite tonality;
- c) brown color by mixing red iron oxides (hematite) with Egyptian blue;
- d) gray colors from the desaturation of the blue color of Egyptian blue by adding small quantities of red iron oxides;
- e) white colors, mainly from calcite, by adding to some of them Egyptian blue to increase the white sensation (low saturation in medium luminosity).

The addition of Egyptian blue to other pigments to provoke a luminosity decrease was also observed. For example, the ocher samples whose color is exclusively obtained from goethite present a higher luminosity than the samples obtained by mixing goethite and Egyptian blue.

We would like to express our gratitude to the *Museo Nacional de Arte Romano* in Mérida, 'Emerita Augusta' (Badajoz, Spain), and especially to *Trinidad Nogales* and *M. Jesús Castellanos* for providing the samples used in this study.

REFERENCES

- [1] J. Riederer, in 'Artists Pigments', Ed. E. W. Fitzhugh, Oxford University Press, New York, 1997, Vol. 3, p. 23.
- [2] D. Ullrich, in 'PACT 17: Datation-Characterisation des peintures pariétales et murales', Eds. F. Delamare, T. Hackens, B. Helly, Rixensart, 1987, p. 323.
- [3] S. Bruni, F. Cariati, F. Casadio, L. Toniolo, *Vib. Spectrosc.* **1999**, *20*, 15.
- [4] W. T. Chase, in 'Science and Archaeology'. Ed. R. H. Brill, MIT Press, Cambridge, Mass., 1971, p. 80.
- [5] S. Bouherour, H. Berke, H.G. Wiedemann, *Chimia* **2001**, *55*, 942.
- [6] H. G. Wiedemann, G. Bayer, *Thermochim. Acta* **1986**, *100*, 283.
- [7] H. G. Wiedemann, G. Bayer, *Chemtech* **1977** (June), 381.
- [8] E. W. FitzHugh, L. A. Zycherman, *Studies in Conservations* **1992**, *37*, 145.
- [9] M. C. Edreira, M. J. Feliu, C. Fernández-Lorenzo, J. Martín, *Analytica Chim. Acta* **2001**, *434*, 331.
- [10] M. C. Edreira, M. J. Feliu, J. Martín, *Caesaraugusta* **1999**, *73*, 263.
- [11] M. C. Edreira, in 'Caracterización químico-física de pinturas murales romanas: Aplicación a La Casa del Mitreo de la ciudad de Mérida (Badajoz)', Ed. Publications Service, University of Cádiz, Cádiz, 1999.
- [12] M. J. Feliu, in 'Aplicación de la Microscopía Electrónica de Barrido a la Arqueometría', Ed. Publications Service, University of Cádiz, Cádiz, 1994.
- [13] A. Mostalac, J. Martín, M. J. Feliu, in 'Análisis por Microscopía Electrónica de Barrido in Colonia Victrix Lula Lepida Celsa (Velilla de Ebro, Zaragoza) Estratigrafías, Pinturas y Cornisas de la Casa de los Delfines. Memoria de las Excavaciones Arqueológicas en Aragón', Diputación General de Aragón, Zaragoza, 1994.

- [14] 'CIE 1964, *Proceedings of 1963*', Committee Report E-1.4.1, Bureau Central de la CIE, Paris.
- [15] R. W. G. Hunt, 'Measuring Colour', 'Ellis Horwood Series in Applied Science and Industrial Technology', London, 1991.
- [16] G. Wyszecki, W. S. Stiles, 'Color Science: Concepts and Methods, Quantitative Data and Formulas', John Wiley & Sons, New York, 1982.
- [17] W. Erb, W. Budde, *Color Res. Applic.* **1979**, *4*, 113.
- [18] F. Delamare, L. Delamare, B. Guineau, G. S. Odin, 'Pigments and Colorants', Éditions du CNRS, Paris, **1990**, p. 103.
- [19] F. Delamare, in 'PACT 17: Datation-Characterisation des peintures pariétales et murales', Eds. F. Delamare, T. Hackens, B. Helly, Rixensart, 1987, p. 345.

Received February 11, 2002